Acknowledgment. We thank L. Monnerie for several helpful comments concerning main-chain motions in polystyrenes. Conclusions about the origins of ring flips in polystyrenes benefited from extended discussions with R. Yaris, J. Skolnick, D. Perchak, and A. Tonelli. This work was supported in part by Grant DMR-8007025 from the Polymer Division of the National Science Foundation.

Registry No. Atactic polystyrene, 9003-53-6; isotactic polystyrene, 25086-18-4; poly(*p*-bromostyrene), 24936-50-3; poly(*p*-chlorostyrene), 24991-47-7; poly(*p*-nitrostyrene), 24936-54-7; poly(*p*-isopropylstyrene, 30872-09-4; poly(α-methylstyrene), 25014-31-7; poly(*o*-bromostyrene), 27290-16-0; poly(*m*-bromostyrene), 25584-47-8; poly(*p*-*tert*-butylstyrene), 26009-55-2.

References and Notes

(1) Schaefer, J.; Sefcik, M. D.; Stejskal, E. O.; McKay, R. A. *Macromolecules*, following paper in this issue.
(2) Stejskal, E. O.; Schaefer, J.; Steger, T. R. *Faraday Soc., Symp.* **1979**, *13*, 56.
(3) Schaefer, J.; Stejskal, E. O.; Steger, T. R.; Sefcik, M. D.; McKay, R. A. *Macromolecules* **1980**, *13*, 1121.
(4) Maricq, M.; Waugh, J. S. *J. Chem. Phys.* **1979**, *70*, 3300.
(5) Hester, R. K.; Ackerman, J. L.; Neff, B. L.; Waugh, J. S. *Phys. Rev. Lett.* **1976**, *36*, 1981.
(6) Stoll, M. E.; Vega, A. J.; Vaughan, R. W. *J. Chem. Phys.* **1976**, *65*, 4093.
(7) Dixon, W. T. *J. Chem. Phys.* **1982**, *77*, 1800.
(8) Munowitz, M. G.; Griffin, R. G.; Bodenhausen, G.; Huang, T. H. *J. Am. Chem. Soc.* **1981**, *103*, 2529.
(9) Munowitz, M. G.; Griffin, R. G. *J. Chem. Phys.* **1982**, *76*, 2848.
(10) Schaefer, J.; McKay, R. A.; Stejskal, E. O.; Dixon, W. T. *J. Magn. Reson.* **1983**, *52*, 123.
(11) Schaefer, J.; Stejskal, E. O.; McKay, R. A.; Dixon, W. T. *Macromolecules*, in press.
(12) Opella, S. J.; Frey, M. H.; DiVerdi, J. A. *J. Magn. Reson.* **1980**, *37*, 165.
(13) Torchia, D. A. *J. Magn. Reson.* **1978**, *30*, 613.
(14) Waugh, J. S.; Huber, L. M.; Haeberlen, U. *Phys. Rev. Lett.* **1968**, *20*, 180.
(15) Haeberlen, U. *Adv. Magn. Reson., Suppl. 1* **1976**, 1.
(16) Herzfeld, J.; Berger, A. E. *J. Chem. Phys.* **1980**, *73*, 6021.
(17) Moore, J. A., Ed. "Macromolecular Syntheses"; Wiley: New York, 1977; Collect. Vol. 1, pp 1-3.
(18) Van, N. B.; Noel, C. *J. Polym. Sci., Polym. Chem. Ed.* **1976**, *14*, 1627.
(19) Cais, R. E.; O'Donnell, J. H.; Bovey, F. A. *Macromolecules* **1977**, *10*, 254.
(20) Cais, R. E.; Bovey, F. A. *Macromolecules* **1977**, *10*, 752.
(21) Tonelli, A. E. *Macromolecules* **1973**, *6*, 682.
(22) See Figure 8 of ref 11.
(23) Hägele, P. C.; Beck, L. *Macromolecules* **1977**, *10*, 213.
(24) Doddrell, D.; Glushko, V.; Allerhand, A. *J. Chem. Phys.* **1972**, *56*, 3683.
(25) McCall, D. W. *Acc. Chem. Res.* **1971**, *4*, 223.
(26) Abragam, A. "The Principles of Nuclear Magnetism"; Oxford University Press: London, 1961; p 565.
(27) In this paper the mean is taken of the square of the sines of the angles rather than the squares of the angles themselves to obtain a root mean square. Arcsin root mean sine square is a more accurate term. For small angles where $\sin\theta \sim \theta$, the two means are the same.
(28) Van Krevalen, D. W. "Properties of Polymers"; Elsevier: New York, 1976; p 267.
(29) Szeverenyi, N. M.; Vold, R. R.; Vold, R. L. *Chem. Phys.* **1976**, *18*, 23.
(30) Stoll, M. E.; Vega, A.; Vaughan, R. W. *J. Chem. Phys.* **1978**, *69*, 5458.
(31) Stark, R. E.; Haberkorn, R. A.; Griffin, R. G. *J. Chem. Phys.* **1978**, *68*, 1996.
(32) Skolnick, J.; Helfand, E. *J. Chem. Phys.* **1980**, *72*, 5489.
(33) Helfand, E. *J. Chem. Phys.* **1971**, *54*, 4651.
(34) Spiess, H. W. *Colloid Polym. Sci.* **1983**, *261*, 193.
(35) Spiess, H. W. *J. Chem. Phys.* **1980**, *15*, 6755.
(36) Spiess, H. W., private communication.
(37) See, for example: McCrum, N. G.; Read, B. E.; Williams, G. "Anelastic and Dielectric Effects in Polymeric Solids"; Wiley: New York, 1967; p 410.
(38) Yano, O.; Wada, Y. *J. Polym. Sci., Part A-2* **1971**, *9*, 669.
(39) Hedvig, P., "Dielectric Spectroscopy of Polymers"; Adam Hilyer, Ltd.: Bristol, 1977; p 114.
(40) Pace, R. J.; Datyner, A. *J. Polym. Sci., Polym. Phys. Ed.* **1979**, *17*, 437.
(41) Sefcik, M. D.; Schaefer, J.; May, F. L.; Raucher, D.; Dub, S. M. *J. Polym. Sci., Polym. Phys. Ed.* **1983**, *21*, 1055.
(42) Light, R. R.; Seymour, R. W. *Polym. Eng. Sci.* **1982**, *22*, 857.
(43) Poly(styrene-*co*-sulfone) is not a systematic name, but rather a convenient representation for the constitution of the polymer whose structural formula is shown in Figure 9.

Carbon-13 $T_{1\rho}$ Experiments on Solid Polymers Having Tightly Spin-Coupled Protons

Jacob Schaefer,* M. D. Sefcik, E. O. Stejskal, and R. A. McKay

Monsanto Company, Physical Sciences Center, St. Louis, Missouri 63167.
Received July 25, 1983

ABSTRACT: A nine-step procedure is established for measuring the cross-polarization transfer rate from protons in local dipolar fields to carbons in an applied radio-frequency field. This measurement permits a determination of the relative contributions of spin and motional dynamics to average carbon rotating-frame relaxation times ($\langle T_{1\rho}(C)\rangle$'s) even in situations when both mechanisms are important. The $\langle T_{1\rho}(C)\rangle$'s at 37 kHz for the methylene carbons of polycrystalline glycine, high-density polyethylene, poly(oxymethylene), and hexadecane contained in a urea clathrate are all dominated by spin dynamics, while those of dipalmitoylphosphatidylcholine, poly(α-methylstyrene), and an atactic melt-quenched polystyrene reflect substantial motional contributions. A phenomenological expression for calculating the cross-polarization transfer rate for methylene carbons in amorphous or polycrystalline materials is also proposed. Calculated values are in reasonable agreement with experiment for nine different solid systems, all of which have tightly spin-coupled protons. In many situations, this simple calculation will permit an estimate of spin–spin contributions to observed carbon rotating-frame relaxation times without elaborate experiments.

Introduction

In a recent discussion of the molecular dynamics of chemically modified polycarbonates, Yee and Smith[1] noted the absence of any clear correlation between the results of dynamic mechanical spectroscopy of these polycarbonates and broad-line proton NMR of the same materials. The source of this difficulty is not hard to find. Molecular motions of the polymer modulate the dipolar interactions on which all NMR relaxation parameters depend. These parameters therefore reflect the inherent

0024-9297/84/2217-1118$01.50/0

long-range dynamic cooperativity of the glassy solid state even through the dipolar interactions themselves are short range. Nevertheless, those motions most responsible for making an observable change in a line width are generally both large-amplitude and high-frequency (upper kilohertz and higher) and may involve only local internal rotations. Such motions may have little to do with the main-chain motion responsible for a mechanical loss. Since the specific molecular origins of a complex *proton* NMR line shape are usually obscure, connections between proton line widths and mechanical loss peaks are equally obscure.

We have proposed a new approach[2] to understanding the microscopic origins of polymer motions in solids and to making a plausible connection between microscopic motions and macroscopic behavior. This approach involves cross-polarization magic-angle ^{13}C NMR.[3] The combination of high-power resonant decoupling[4] and high-speed sample rotation at the magic-angle[5] produces a ^{13}C NMR spectrum with liquid-like resolution so that chemically different carbons can be identified by separate resonances. This high-resolution technique becomes a high-sensitivity one when combined with the cross-polarization of magnetization from abundant to rare spins.[6]

The high resolution of the cross-polarization magic-angle spinning experiment means that the relaxation properties of chemically different types of carbons can be examined individually. This simplification removes much of the obscurity as to the molecular origins of the motions responsible for carbon dipolar line widths,[7,8] chemical shift tensors,[9-11] and T_1 and $T_{1\rho}$ spin–lattice relaxation rates.[12,13] The same clarity of analysis is possible for proton NMR only with specific deuterium labeling. In addition, the carbon relaxation parameters are free from the averaging effects of spin diffusion, and this too aids in the identification of the particular motion responsible for relaxation. As a result, it has been possible, for example, to correlate $T_{1\rho}$(C)'s (resulting from mid-kilohertz main-chain restricted motions) with both structural and physical modifications of polycarbonates,[14] poly(ethylene terephthalates),[15] and polystyrenes.[16] Such connections are not completely unexpected, since low-frequency main-chain motions have long been linked to ultimate mechanical properties.[17] Nevertheless, the success of this empiricism emphasizes the importance of carbon $T_{1\rho}$ measurements.

There is a complication in the use of these ^{13}C $T_{1\rho}$'s, however. The possibility exists[2] of static ^1H–^{13}C spin–spin interactions shortening $T_{1\rho}$(C) and so confusing its quantitative interpretation as a motional parameter. We have demonstrated[12,18] that the ambiguity associated with this complication can be removed by a direct measurement of the cross-polarization transfer rate, T_{IS}^{-1}(ADRF), from protons in the local dipolar field to carbons in the applied field, H_1(C). A comparison of $T_{1\rho}$(C) with T_{IS}(ADRF) then establishes quantitatively any contribution of spin dynamics to $T_{1\rho}$(C).

We have applied this procedure before to glassy polymers such as, for example, polycarbonate[14] and poly(ethylene terephthalate).[15] It was easy to establish in these two cases that $T_{1\rho}$(C) was dominated by contributions from molecular dynamics for H_1(C)'s of about 30 kHz because the differences between $T_{1\rho}$(C) and T_{IS}(ADRF) were large. To extract useful information on molecular dynamics from $T_{1\rho}$(C) when this difference is not large requires that both relaxation parameters be measured with accuracy. In this paper we report developments that substantially improve our ability to measure T_{IS}(ADRF). In addition, we specify procedures by which reliable values for T_{IS}(ADRF) can be calculated. We then compare observed and calculated T_{IS}(ADFR)'s with $T_{1\rho}$(C)'s for a variety of amorphous and polycrystalline polymers, all of which have rigid, tightly spin-coupled protons, and indicate for which systems $T_{1\rho}$(C) contains useful information on molecular dynamics.

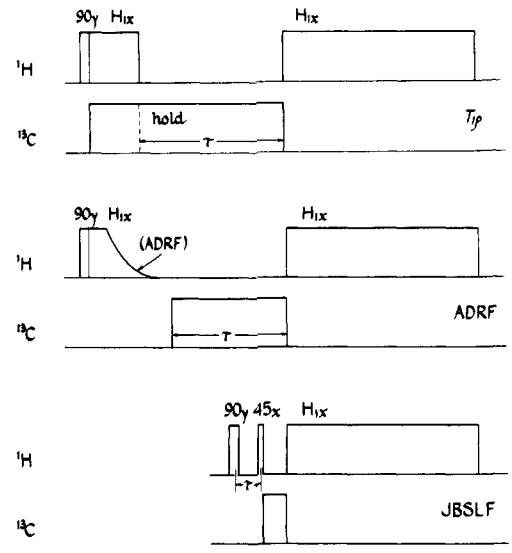

Figure 1. Pulse sequences for three cross-polarization experiments.

Experiments

Carbon-13 cross-polarization NMR experiments were performed at 22.6 and 15.1 MHz with spectrometers described before.[8,19] The pulse sequences employed in these experiments are shown in Figure 1. In the first experiment, following a matched, spin-lock Hartmann–Hahn generation of a carbon polarization,[6] the proton radio-frequency field was turned off abruptly. After a 50-μs delay, a linear fit to the steady-state rate of decay of the total carbon magnetization held in its rotating field for the next millisecond yielded $\langle T_{1\rho}(C)\rangle$, the average carbon spin-lock lifetime.[8] This experiment was performed on spinning samples only.

In the second experiment illustrated in Figure 1, following a spin locking of the protons, the ^1H radio-frequency field was turned off in times of about 0.5 ms (long compared to proton T_2's), so that the order established by the spin lock was transferred to the local dipolar field.[20] This process is called an adiabatic demagnetization in the rotating frame (ADRF). The shape of the demagnetizing pulse was controlled by an arbitrary waveform generator. An estimate of the initial rate of nontransient polarization transfer from the local field to the ^{13}C radio-frequency field, $(dS/dt)_{t=0}$, was made with the time $t = 0$ defined as 50 μs after the application of the carbon radio-frequency field. This rate was used to derive[18] the average ADRF cross-polarization time constant, $\langle T_{IS}(ADRF)\rangle$. These measurements were performed only on stationary (nonspinning) samples to avoid perturbing the orientation of the ^1H–^1H internuclear vectors relative to the applied static magnetic field and so shortening $\langle T_{IS}(ADRF)\rangle$.[21]

In the third experiment illustrated in Figure 1, a pair of Jeener-Broekaert (JB) phase-shifted proton radio-frequency pulses generated dipolar order along local proton dipolar fields.[22] The order established by the two-pulse sequence, as a function of the effective spacing between pulses, τ, was then immediately read by a transient cross-polarization transfer using an 8-μs carbon radio-frequency pulse.[23] The intensity of each high-resolution carbon resonance (as a function of the proton pulse spacing) became a measure of the derivative of the free induction decay of the proton line shape of a particular class, or chemical type of proton. Average proton separated local fields were determined directly from the individual intensity maxima since[23] $H_L = 1/(2\pi 3^{1/2}\tau_{max})$. This experiment, designated JBSLF, was performed on spinning samples with all pulse widths small compared to the rotor period.

The H_1(C)'s used in these experiments were calibrated by measuring 360° pulse lengths. Voltages at the coil generated by

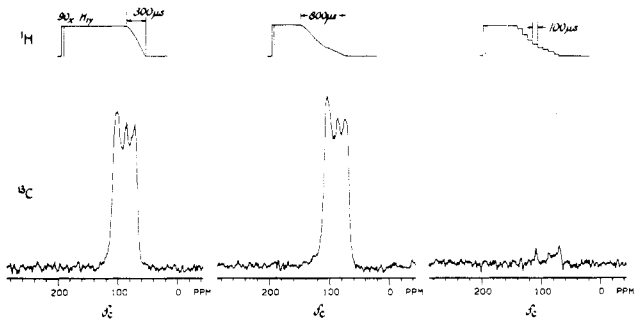

Figure 2. 15.1-MHz ^{13}C magnetization of poly(oxymethylene) arising from a 10-ms transfer from protons in their local field. The pulse sequence of Figure 1 (middle) was used with $H_1(C)$ = 37 kHz, together with a variety of schemes for the demagnetization of the protons. The nonspinning truncated sample was approximately two-thirds the height of the double-tuned radio-frequency coil.

long pulses varied linearly with $H_1(C)$'s calibrated by short pulses.

All of the materials used in these experiments are commercially available, with the exception of the completely alternating copolymer, $-(CHPhCH_2SO_2)_n-$, which was supplied by Dr. R. E. Cais of Bell Laboratories. A hexadecane–urea clathrate was prepared by the procedure described by Schiessler and Flitter.[24]

Results

A variety of schemes for the removal of the proton radio frequency in ADRF experiments was examined. As long as abrupt changes in $H_1(H)$ were avoided, the dipolar order established by various rates of change in $H_1(H)$ (all less than T_2^{-1} of the protons but greater than any other relaxation or transfer rate present) resulted in about the same 10-ms cross-polarization transfer to carbons (Figure 2). This implies the efficiency of the ADRF process is not overly sensitive to the way $H_1(H)$ is removed. A smoothly decreasing $H_1(H)$ program (Figure 2, middle) with about a 100-ms time constant was adopted for all remaining ADRF measurements.

For a ridid crystalline material such as glycine, we know[8] that $T_{1\rho}(C) = T_{IS}(ADRF)$. Thus, for the experiment of Figure 1 (middle)

$$\left(\frac{dS}{dt}\right)_{t=0} = \frac{S_0 - S_i}{\langle T_{IS}(ADRF)\rangle} \tag{1}$$

where $(dS/dt)_{t=0}$ is the initial rate of nontransient polarization transfer from protons to carbons,[18] S_i is the carbon polarization developed during the transient, $\langle T_{IS}(ADRF)\rangle$ is the *average* ADRF cross-polarization time constant, and

$$S_0 = S_m(\gamma_C H_1(C)/\gamma_H H_L)\epsilon \tag{2}$$

In eq 2, S_m is the carbon polarization developed in a matched spin-lock cross-polarization transfer with no dissipative processes, $H_1(C)$ is the carbon radio-frequency field, γ_C and γ_H are the carbon and proton gyromagnetic ratios, respectively, ϵ is the efficiency of the ADRF process, and H_L is the average proton local dipolar field. The glycine proton local field, H_L, was measured[23] as 9.2 kHz in a JBSLF experiment.

For a matched spin-lock transfer generating an observed carbon polarization, S_{obsd}, we have (assuming the transfer rate is much greater than the rate of decay of the spin-locked protons)

$$S_m = S_{obsd} \exp(\tau/T_{1\rho}(H)) \tag{3}$$

where τ is the transfer time (generally 1–2 ms; this is sufficient to produce representative intensities for all carbons in polymers) and $T_{1\rho}(H)$ is the proton rotating-frame relaxation time.[6] Thus, $\langle T_{IS}(ADRF)\rangle$ for glycine can be determined as a function of ϵ by measuring $(dS/dt)_{t=0}$, S_i, S_{obsd}, and $T_{1\rho}(H)$ and using eq 1–3 with H_L = 9.2 kHz.

Table I
$\langle T_{IS}(ADRF)\rangle^a$ for the Methylene Carbons of Glycine as a Function of the Efficiency (ϵ) of the ADRF Process for Two Values of $H_1(C)$

	$H_1(C)$, kHz	
ϵ	28	37
0.50	1.73	7.12
0.60	2.07	8.55
0.65	2.25	9.26
0.70	2.42	9.97
0.80	2.77	11.39
0.90	3.12	12.82
1.00	3.46	14.24

[a] From eq 1 and 2.

Table II
Methylene-Carbon $\langle T_{1\rho}(C)\rangle$'s[a] (ms) as a Function of $H_1(C)$

	$H_1(C)$, kHz			
system	28	37	44	54
glycine	2.7	9.7	27	70
dipalmitoyl-phosphatidylcholine	4.1	11.0	25	82

[a] From magic-angle spinning $T_{1\rho}(C)$ experiments; linear fit to decay from 0.05 to 1.0 ms after removal of $H_1(H)$.

The dependence of $\langle T_{IS}(ADRF)\rangle$ on ϵ for polycrystalline glycine is shown in Table I for two values of $H_1(C)$. For ϵ between 0.7 and 0.8, the value of $\langle T_{IS}(ADRF)\rangle$ is about equal to that of $\langle T_{1\rho}(C)\rangle$ for both $H_1(C)$ = 28 and 37 kHz (Table II). In all subsequent measurements, we choose ϵ = 0.8.

For glycine, the ADRF transfer for longer cross-polarization times, t, generates a carbon magnetization, S, given by[18]

$$S = S_i \exp(-t/\langle T_{IS}(ADRF)\rangle) + \frac{S_0}{\langle T_{IS}(ADRF)\rangle} \frac{\exp(-t/T_{1\rho}) - \exp(-t/\langle T_{IS}(ADRF)\rangle)}{1/\langle T_{IS}(ADRF)\rangle - 1/T_{1D}} \tag{4}$$

where the only new parameter is T_{1D}, which we measured in a separate experiment[18] as 45 ms. We take the orientational dependence of $T_{IS}(ADRF)$ for a polycrystalline sample into account by assuming, as before,[18]

$$\langle T_{IS}(ADRF)\rangle^{-1} = f_a/T_{IS,a} + f_b/T_{IS,b} \tag{5}$$

where

$$f_a = 0.85; \qquad f_b = 0.15$$

and

$$T_{IS,a} = 10T_{IS,b}$$

Calculated ADRF transfer curves using eq 5 are in reasonable agreement with experiment for both $H_1(C)$ = 28 and $H_1(C)$ = 37 kHz (Figure 3). This agreement supports our procedures for establishing ϵ and H_L as well as our ability to compare $\langle T_{1\rho}(C)\rangle$ measured in a magic-angle spinning experiment with a $\langle T_{IS}(ADRF)\rangle$ measured in a nonspinning experiment.

We followed a nine-step procedure for measuring $\langle T_{IS}(ADRF)\rangle$ for methylene carbons in a polymer for which it is not clear that $\langle T_{IS}(ADRF)\rangle = \langle T_{1\rho}(C)\rangle$. First we measured S_{obsd} by a standard matched spin-lock cross-polarization transfer *without* magic-angle spinning. The methylene carbon of interest represents a known fraction of the observed magnetization. For example, for poly(α-methylstyrene) the methylene-carbon intensity is $^1/_9$ that observed (Figure 4), while for poly(*o*-bromo-

Table III
Methylene-Carbon Relaxation Parameters ($H_1(C) = 37$ kHz)

system[a]	$\langle T_{1\rho}(C)\rangle$,[b] ms	$\langle T_{IS}(ADRF)\rangle_{obsd}$,[c] ms	$\langle T_{IS}(ADRF)\rangle_{calcd}$,[d] ms	$H_L(H)$,[e] kHz
glycine	9.7	11.4		9.2
polyethylene (high density)	2.7	3.0	4.2	10.8
poly(oxymethylene) (75% crystalline)	10.5	9.7	10.0	9.2
dipalmitoyl-phosphatidylcholine	11.0	23	19.3	8.3
hexadecane (urea clathrate)	27.5	38	36.2	7.6
poly(α-methylstyrene)	2.5	6.1	7.4	9.7

[a] Polycrystalline or amorphous materials at $T = 26$ °C. [b] From magic-angle spinning $T_{1\rho}(C)$ experiments; linear fit to decay from 0.05 to 1.0 ms after removal of $H_1(H)$. [c] From eq 6 with $\epsilon = 0.8$. [d] Relative to a glycine 10-ms value, using eq 8 and experimental values of $H_L(H)$. [e] From Jeener-Broekaert separated local field experiments.

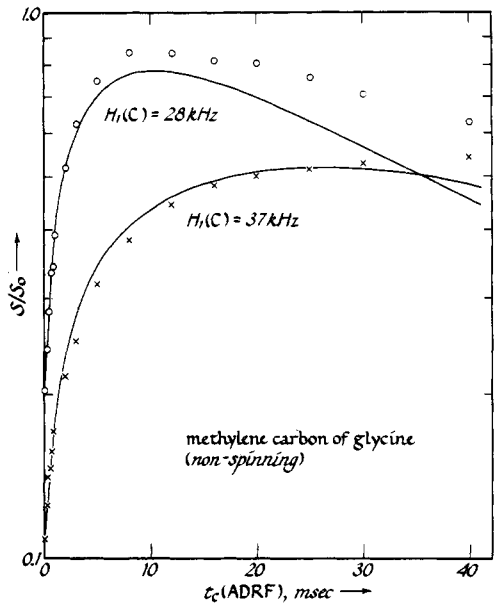

Figure 3. Evolution of 15.1-MHz ^{13}C magnetization in the experiment of Figure 1 (middle) for a stationary truncated sample of polycrystalline glycine using two values of $H_1(C)$. Circles and crosses indicate experimental values and solid lines calculations using eq 4 as described in the text.

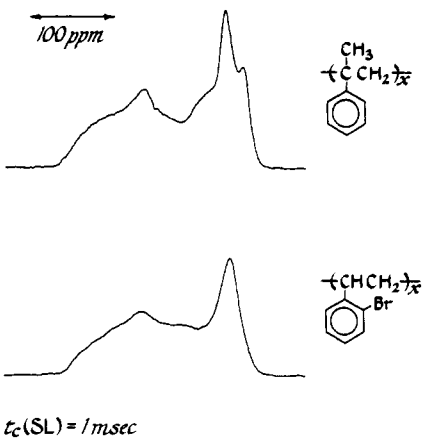

Figure 4. 22.6-MHz ^{13}C NMR spectra arising from a conventional 1-ms 37-kHz matched spin-lock cross-polarization transfer for two stationary truncated amorphous materials, poly(α-methylstyrene) (top) and poly(*o*-bromostyrene) (bottom).

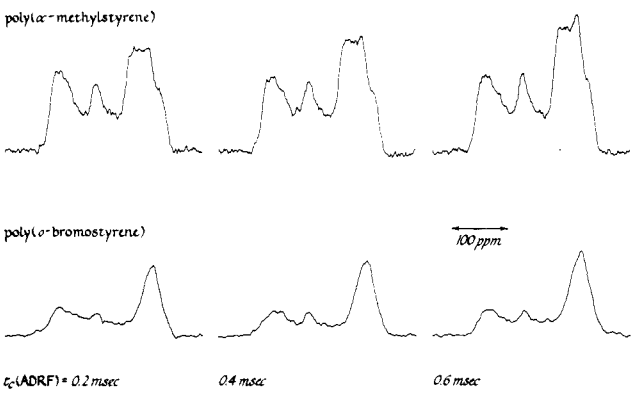

Figure 5. 22.6-MHz ^{13}C NMR spectra from the experiment of Figure 1 (middle) for two polymers. Only short contact times are used in this determination of $(dS/dt)_{t=0}$ as described in the text associated with eq 6.

styrene), it is $^1/_7$ (the bromonated aromatic-carbon intensity is missing[17] because of dipolar broadening to a quadrupolar nucleus[12,25]). Second, we measured $T_{1\rho}(H)$ from a matched spin-lock cross-polarization experiment. It is immaterial whether this is done with or without spinning. For long contact times, the carbon magnetization tracks the $T_{1\rho}$ decay of the proton magnetization with which it is in thermal equilibrium.[26] Next, we determined S_m using eq 3. We then performed a JBSLF experiment which determines the H_L for the methylene protons. The fifth step in the procedure was to calculate S_0 by using eq 2 with the known values of S_m, H_L, and $H_1(C)$ and with $\epsilon = 0.8$. The sixth step was to determine S_i, which we did by measuring the transient transfer in a nonspinning ADRF experiment (Figure 1, middle, with a contact time of 100 μs) for all the carbons of the polymer, taking the fraction of this intensity represented by the methylene carbon as established in the high-resolution JBSLF experiment. For poly(α-methylstyrene), for example, the single methylene carbon accounts for 22% of S_i.[23] The seventh step was to measure $(dS/dt)_{t=0}$ (on the same intensity scale as used to measure S_{obsd}). We made the reasonable assumption that for short ADRF transfer times (200–600 μs) only transfers to protonated carbons with minor internal motion are significant.[23] Thus $(dS/dt)_{t=0}$ for the methylene carbons of poly(α-methylstyrene), for example, can be obtained from the total increase in intensity in the aliphatic region of the spectrum (Figure 5, top). The corresponding increase for poly(*o*-bromostyrene) must be attributed to both methine and methylene carbons (Figure 5, bottom). The eighth step was to measure $\langle T_{1\rho}(C)\rangle$ with spinning. Finally, we computed $\langle T_{IS}(ADRF)\rangle$ using the relationship[18]

$$(dS/dt)_{t=0} = S_0/\langle T_{IS}(ADRF)\rangle - S_i/\langle T_{1\rho}(C)\rangle \quad (6)$$

Values of $\langle T_{IS}(ADRF)\rangle$ determined this way for the methylene carbons of a variety of systems are presented in Table III, along with values for the corresponding

Table IV
Main-Chain Aliphatic Carbon Relaxation Parameters (H_1(C) = 37 kHz)

polymer	$\langle T_{1\rho}(C)\rangle$,[a] ms	$\langle T_{IS}(ADRF)\rangle_{obsd}$,[b] ms	$\langle T_{IS}(ADRF)\rangle_{calcd}$,[c] ms	$H_L(H)$,[d] kHz
polystyrene	8.0	24	40	7.5
polystyrene-*co*-sulfone $-(CH_2CHPhSO_2)_x-$	18.0	34	27	7.9
poly(*o*-bromostyrene)	5.2	20	40	7.5

[a] From magic-angle spinning $T_{1\rho}$(C) experiments; linear fit to decay from 0.05 to 1.0 ms after removal of H_1(H). [b] From eq 6 with ϵ = 0.8. [c] Relative to a glycine 10-ms value, using eq 9 and experimental values of H_L(H). [d] From Jeener-Broekaert separated local field experiments.

Table V
$\langle T_{1\rho}(C)\rangle$[a] (ms) for Poly($\alpha$-methylstyrene) as a Function of H_1(C)

carbon	H_1(C), kHz 37	44	54	60
methylene	2.5	6.6	21	45
methyl	6.1	6.3	6.4	7.0
quaternary (main chain)	27	49	125	320
aromatic (protonated)	19	47	75	145

[a] From magic-angle spinning $T_{1\rho}$(C) experiments; linear fit to decay from 0.05 to 1.0 ms after removal of H_1(H).

Table VI
Field Dependence of Main-Chain $\langle T_{1\rho}(C)\rangle$'s[a] (ms) for Two Polystyrenes

polymer	carbon	H_1(C), kHz 37	44	54	60
melt-quenched atactic polystyrene	methine[b]	12	30	52	81
isotactic polystyrene,[c] precipitated from decalin	methylene	10	24	54	160

[a] From straight-line fit to decay between 0.05 and 1.0 ms after removal of H_1(H) unless $\langle T_{1\rho}(C)\rangle$ was greater than 100 ms, in which case decay time was extended to 10% loss point. [b] From deconvolution of aliphatic-carbon resonance. [c] Poly(styrene-α-*d*), greater than 95% isotactic.

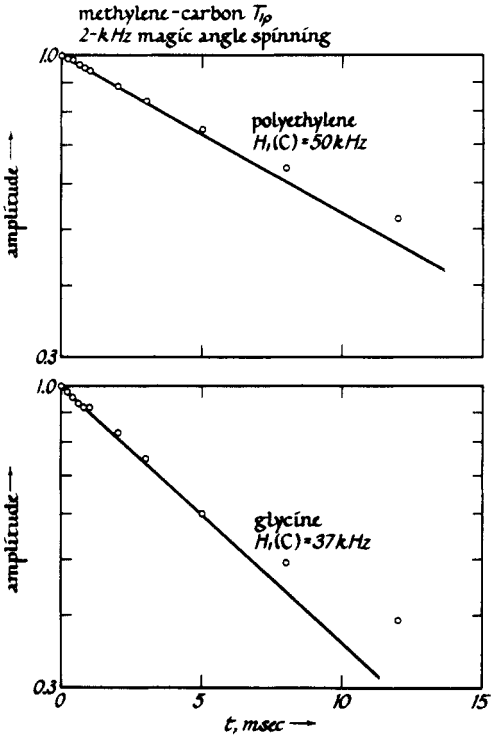

Figure 6. 15.1-MHz $T_{1\rho}$(C) plots for two polycrystalline materials. The first data point of each relaxation curve was acquired 50 μs following removal of the proton radio-frequency field (Figure 1, top).

$\langle T_{1\rho}(C)\rangle$'s and H_L's. Values of $\langle T_{IS}(ADRF)\rangle$ for the unresolved resonances of aliphatic main-chain carbons of three polystyrenes are presented in Table IV.

The determination of $\langle T_{1\rho}(C)\rangle$ has been described in detail before.[12] Standard procedures were used for the values reported in Tables II–VI. The quality of the relaxation data is illustrated in Figure 6 for polyethylene (top) and glycine (bottom). Both plots show a minor nonlinearity which, for these rigid materials, we attribute to incomplete spatial averaging under magic-angle spinning (cf. below). The H_1(C) dependencies of $\langle T_{1\rho}(C)\rangle$'s are reported for the methylene carbons of glycine and dipalmitoylphosphatidylcholine (Table II) as well as for several different carbons of poly(α-methylstyrene) (Table V) and main-chain carbons of two polystyrenes (Table VI).

Discussion

Comparisons of $\langle T_{1\rho}(C)\rangle$ and $\langle T_{IS}(ADRF)\rangle$. The ratio of $\langle T_{1\rho}(C)\rangle$ to $\langle T_{IS}(ADRF)\rangle$ determines the extent of spin–spin contributions to $\langle T_{1\rho}(C)\rangle$.[12,18] If this ratio is close to 1, $\langle T_{1\rho}(C)\rangle$ is dominated by spin dynamics. If the ratio is close to 0, $\langle T_{1\rho}(C)\rangle$ is dominated by molecular dynamics. Examination of Table III shows that $\langle T_{1\rho}(C)\rangle$ at 37 kHz for the methylene carbons of glycine, polyethylene, and poly(oxymethylene) is dominated by contributions from spin dynamics since $\langle T_{1\rho}(C)\rangle$'s and $\langle T_{IS}$(ADRF)$\rangle$'s are equal, within the approximately 10% experimental error. This equality may also hold for the hexadecane–urea cathrate, despite the known extensive rotational motion of hexadecane about the axis of the crystal channel.[27] However, there are clearly substantial motional contributions to $\langle T_{1\rho}(C)\rangle$ for both dipalmitoylphosphatidylcholine and poly(α-methylstyrene) as well as for all three of the polystyrenes of Table IV.

These conclusions would be difficult to reach based solely on the H_1(C) dependence of $\langle T_{1\rho}(C)\rangle$. Except for the unusual situation where $\langle T_{1\rho}(C)\rangle$ is virtually independent of H_1(C), such as, for example, is true for the relaxation of the α-methyl carbon of poly(α-methylstyrene) (Table V), the H_1(C) dependence of $\langle T_{1\rho}(C)\rangle$ can be misleading. For example, the H_1(C) dependences of the methylene-carbon $\langle T_{1\rho}(C)\rangle$'s of both dipalmitoylphosphatidylcholine and glycine are about the same (Table II). This occurs, however, not because both $\langle T_{1\rho}(C)\rangle$'s are equally dominated by spin–spin effects but rather because the proton local field of dipalmitoylphosphatidylcholine is less than that of glycine. This leads to a stronger H_1(C) dependence for the spin–spin contribution to the $\langle T_{1\rho}(C)\rangle$ of dipalmitoylphosphatidylcholine, which masks the weaker dependence of the motional component, in the H_1(C) regime where contributions from both components are important.

A second complication in the use of $H_1(C)$ dependence of $\langle T_{1\rho}(C)\rangle$'s results from the choice of method of determining the initial slope of a $T_{1\rho}(C)$ plot. We have knowingly adopted a conservative method consisting of a linear fit to the decay over a full millisecond.[8] For systems with minor (but still measurable) motional contributions to $T_{1\rho}(C)$, the initial part of the $T_{1\rho}(C)$ decay may be decidedly nonlinear, but only for a time comparable to the short correlation time of the motion responsible for the relaxation.[28] For polymers such as polystyrenes this time can be of the order of 100 μs. If the remainder of the $T_{1\rho}(C)$ decay is slow (as it is at higher H_1's), the true average $T_{1\rho}(C)$ can be misrepresented by our sampling technique and $\langle T_{1\rho}(C)\rangle$ will be overestimated. The degree of this misestimate depends on the overall shape of the $T_{1\rho}(C)$ plot and so becomes worse with increasing $H_1(C)$. Woessner has considered a similar problem in analysis of nonlinear T_1 plots for systems having multiple T_1's partially averaged by exchange.[28] Complications occur when the exchange rate is comparable to one of the shorter T_1's. For $T_{1\rho}(C)$'s an analogous complication occurs[29] when the correlation time for molecular motion is comparable to a local $T_{1\rho}(C)$.

In general, the $H_1(C)$ dependence of a spin–spin contribution to $\langle T_{1\rho}(C)\rangle$ is difficult to predict quantitatively since it depends on subtle details of the tail of a dipolar fluctuation spectrum, possibly modified by molecular motion. Nevertheless, useful qualitative information can often be inferred from comparisons of $H_1(C)$ dependences of similar systems. For example, the approximate equivalence of the $T_{1\rho}(C)$ at 37 kHz of the methine carbon of atactic polystyrene with that of the doubly protonated methylene carbon of a partially crystalline polystyrene *and* the weaker $H_1(C)$ dependence of the methine-carbon $\langle T_{1\rho}(C)\rangle$ (Table VI) are only consistent with the greater importance of spin–lattice processes for the atactic polystyrene system.

Calculated $\langle T_{IS}(ADRF)\rangle$'s. Cheung and Yaris[30] have offered a theoretical prescription for calculating T_{IS}(ADRF). Assuming a single H_L (all protons uniformly tightly coupled), they find for a methylene carbon

$$T_{IS}(ADRF) = 0.000265H_L \exp(3^{1/2}H_1(C)/H_L) \quad (7)$$

where H_L is expressed in kilohertz and $T_{IS}(ADRF)$ in ms. Using eq 7 and the 9.2-kHz H_L of glycine, we calculate a methylene-carbon glycine $T_{IS}(ADRF)$ of 2.5 ms at 37 kHz, about a factor of 4 less than observed (Table III). In addition, the $H_1(C)$ dependence predicted by eq 7 is in poor agreement with experiment (Table II). A semilogarithmic plot of $\langle T_{IS}(ADRF)\rangle$ (which equals $\langle T_{1\rho}(C)\rangle$) as a function of $H_1(C)$ yields from the slope a value of H_L of 13.5 kHz, too large by more than 4 kHz.

We feel the difficulty is in the assumption of a single H_L. Protons in different crystallites certainly do not communicate, and even in amorphous materials local packing variations can restrict proton–proton spin communication. Thus, different local fields will persist in the solid for different proton–proton internuclear orientations with respect to H_0. A broad-line proton NMR experiment or a JBSLF experiment yields a properly weighted average value for the local field. But an observed $\langle T_{IS}(ADRF)\rangle$ is an average of $T_{IS}(ADRF)$'s and not a $T_{IS}(ADRF)$ from an average H_L.

Garroway and VanderHart[13] determined an H_L of 11.5 kHz for a particular oriented crystalline polyethylene. Use of their single value also leads to difficulties in analyzing powder average $\langle T_{IS}(ADRF)\rangle$'s. At $H_1(C)$ = 50 kHz, for an H_L of 11.5 kHz, we compute a $T_{IS}(ADRF) = T_{1\rho}(C)$ of 2 ms while we observe a value of about 16 ms for the polycrystalline material (Figure 6, top), almost an order of magnitude longer.

The anomalous $H_1(C)$ dependence of the glycine $T_{1\rho}(C)$ discussed above may also be interpretable in terms of a distribution of local fields. For large $H_1(C)$, the biggest contributors to $\langle T_{IS}(ADRF)\rangle^{-1}$ are those crystallites with large H_L's. Thus deriving an H_L from a limited $T_{IS}(ADRF)$ radio-frequency field dependence will always lead to a misrepresentative value since the smaller H_L's will be discriminated against.

Phenomenological Estimates of $\langle T_{IS}(ADRF)\rangle$ for Methylene Carbons. We have discovered, in estimating $\langle T_{IS}(ADRF)\rangle$'s for methylene carbons, we can take powder orientation effects into account phenomenologically by using eq 7, but by computing values *relative* to a known rigid-lattice polycrystalline value. That is

$$\langle T_{IS}(ADRF)\rangle = [H_L/H_L^{ref}] \times \langle T_{IS}^{ref}(ADRF)\rangle \exp\{3^{1/2}H_1(C)[H_L^{ref} - H_L]/H_LH_L^{ref}\} \quad (8)$$

where the superscript refers to the reference compound. We select a reference as similar in spin-dynamic properties to our analytical sample as possible. For example, using a 10-ms $\langle T_{IS}(ADRF)\rangle$ at 37 kHz for the methylene carbons of glycine as reference, for other methylene carbons we propose

$$\langle T_{IS}(ADRF)\rangle = 1.09H_L \exp[7.0(9.2 - H_L)/H_L] \text{ (ms)} \quad (9)$$

with the relevant methylene proton local field H_L expressed in kilohertz and $H_1(C)$ = 37 kHz. Values calculated this way are presented in Tables III and IV and appear in reasonable agreement with experiment, especially for those systems in which $\langle T_{IS}(ADRF)\rangle$ clearly arises exclusively from methylene carbons.

Equation 8 can be used at other $H_1(C)$'s as well. Taking glycine as a reference again, but now with $H_1(C)$ = 50 kHz and $T_{IS}^{ref}(ADRF)$ = 60 ms, we predict a $T_{IS}(ADRF)$ for high-density polyethylene of 17 ms, in good agreement with the observed value of 15 ms (Figure 6).

This agreement may seem a little surprising at first. For a methylene carbon, $T_{IS}(ADRF)$ depends on both the CH and HH orientations with respect to H_0.[20,31] The latter determines the various H_L's. In evaluating theoretical expressions for $\langle T_{IS}(ADRF)\rangle$, a spatial powder average over CH orientations cannot be performed independently of the average over HH orientations since the two are correlated. Nevertheless, the accurate predictions of the calculated methylene-carbon $\langle T_{IS}(ADRF)\rangle$'s of Table III suggest that just such an independent average is possible. We suspect the basis for this success lies in the fact that for any given CH direction most HH directions occur in the powder. Thus, the two spatial averages are at least approximately independent. A change in H_L from one polymer to the next produces only a simple change in scale for $\langle T_{IS}(ADRF)\rangle$'s.

We have seen manifestations of this sort of spatial averaging in at least two other types of measurements: first, in the representative proton line shapes generated by *un*representative proton–carbon transient cross-polarization transfers in JBSLF experiments,[23] and second, in the almost linear $T_{1\rho}(C)$ plots of Figure 6. In the latter situation, for polycrystalline polyethylene and glycine, $T_{1\rho}(C)$ equals $\langle T_{IS}(ADRF)\rangle$ so that there is no contribution of dynamic heterogeneity[2,8,32] to a $T_{1\rho}(C)$ plot. For each CH orientation in the static solid, magic-angle spinning (with rotation period short compared to $\langle T_{1\rho}(C)\rangle$) produces a cone on which spatial averaging occurs. For the entire sample, spinning produces a collection of cones, each with its own $T_{1\rho}$. These individual $T_{1\rho}(C)$'s cannot differ significantly, however, because the observed $T_{1\rho}(C)$ plots are

nearly linear. The different spatial averages are all about the same. Only a few special orientations may not fit this averaging pattern, thereby resulting in a slight curvature. That is, nonlinearity in $T_{1\rho}(C)$ can arise from contributions from those methylene carbons having a carbon–proton internuclear vector lying along the sample rotation axis. Carbons approximately satisfying this condition will have relatively long $T_{1\rho}(C)$'s which will remain longer than the average for the whole sample even with magic-angle spinning.

Regardless of the details of the orientational averaging, the observation remains that relative methylene-carbon $\langle T_{IS}(ADRF)\rangle$'s can be calculated if the corresponding H_L's are known. This means estimates of spin–spin contributions to methylene-carbon $\langle T_{1\rho}(C)\rangle$'s for any polymer can be made without recourse to elaborate nine-step ADRF procedures. A proton T_2 or a JBSLF determination of H_L, in combination with the use of eq 8, may be sufficient. The more elaborate accurate determination of the ratio of $\langle T_{1\rho}(C)\rangle$ to $\langle T_{IS}(ADRF)\rangle$ can then be reserved for particularly difficult cases.

Estimates of $\langle T_{IS}(ADRF)\rangle$ for other types of carbons are also possible. Thus, the 7-kHz H_L for the protonated aromatic carbon of poly(α-methylstyrene)[23] suggests a $\langle T_{IS}(ADRF)\rangle$ of about 70 ms (eq 9). A more accurate estimate would probably result if parameters from an aromatic reference compound were used in eq 9 rather than those from glycine. Nevertheless, it is clear that the observed $\langle T_{1\rho}(C)\rangle$ at 37 kHz of 19 ms (Table V) must be dominated by spin–lattice contributions.

Registry No. Glycine, 56-40-6; polyethylene (homopolymer), 9002-88-4; dipalmitoylphosphatidylcholine, 2644-64-6; poly(α-methylstyrene) (homopolymer), 25014-31-7; polystyrene (homopolymer), 9003-53-6; hexadecane–urea clathrate, 3311-88-4; poly(*o*-bromostyrene) (homopolymer), 27290-16-0; isotactic polystyrene (homopolymer), 25086-18-4.

References and Notes

(1) Yee, A. F.; Smith, S. A. *Macromolecules* **1981**, *14*, 54.
(2) Schaefer, J.; Stejskal, E. O.; Buchdahl, R. *Macromolecules* **1977**, *10*, 384.
(3) Schaefer, J.; Stejskal, E. O. *J. Am. Chem. Soc.* **1976**, *98*, 1030.
(4) Bloch, F. *Phys. Rev.* **1958**, *11*, 841.
(5) Andrew, E. R.; Bradbury, A.; Eades, R. G. *Nature (London)* **1958**, *182*, 1659.
(6) Pines, A.; Gibby, M. G.; Waugh, J. S. *J. Chem. Phys.* **1973**, *59*, 569.
(7) Hester, R. K.; Ackerman, J. L.; Neff, B. L.; Waugh, J. S. *Phys. Rev. Lett.* **1976**, *36*, 1081.
(8) Schaefer, J.; McKay, R. A.; Stejskal, E. O.; Dixon, W. T. *J. Magn. Reson* **1983**, *52*, 123.
(9) Maricq, M.; Waugh, J. S. *J. Chem. Phys.* **1979**, *70*, 3300.
(10) Herzfeld, J.; Berger, A. E. *J. Chem. Phys.* **1980**, *73*, 6021.
(11) Stejskal, E. O.; Schaefer, J.; McKay, R. A. *J. Magn. Reson.* **1978**, *25*, 569.
(12) Schaefer, J.; Stejskal, E. O.; Steger, T. R.; Sefcik, M. D.; McKay, R. A. *Macromolecules* **1980**, *13*, 1121.
(13) VanderHart, D. L.; Garroway, A. N. *J. Chem. Phys.* **1979**, *71*, 2772.
(14) Steger, T. R.; Schaefer, J.; Stejskal, E. O.; McKay, R. A. *Macromolecules* **1980**, *13*, 1127.
(15) Sefcik, M. D.; Schaefer, J.; Stejskal, E. O.; McKay, R. A. *Macromolecules* **1980**, *13*, 1132.
(16) Schaefer, J.; Sefcik, M. D.; Stejskal, E. O.; McKay, R. A.; Dixon, W. T.; Cais, R. E. *ACS Symp. Ser.* **1984**, *No. 247*, 43.
(17) See, for example: Boyer, R. F. In "Polymeric Materials"; American Society for Metals: Metals Park, OH, 1975; p 277.
(18) Stejskal, E. O.; Schaefer, J.; Steger, T. R. *Faraday Symp. Chem. Soc.* **1979**, *13*, 56.
(19) Schaefer, J.; Stejskal, E. O. *Top. Carbon-13 NMR Spectrosc.* **1979**, *3*, 284.
(20) McArthur, D. A.; Hahn, E. L., Walstadt, R. E. *Phys. Rev.* **1969**, *188*, 609.
(21) Pourquié, J. F. M. M.; Wind, R. A. *Phys. Lett.* **1976**, *55A*, 347.
(22) Jeener, J.; Broekaert, P. *Phys. Rev.* **1967**, *157*, 232.
(23) Schaefer, J.; Sefcik, M. D.; Stejskal, E. O.; McKay, R. A. *Macromolecules* **1981**, *14*, 280.
(24) Schiessler, R. W.; Flitter, D. *J. Am. Chem. Soc.* **1952**, *74*, 1720.
(25) Stoll, M. E.; Vaughn, R. W.; Saillant, R. B.; Cole, T. J. *Chem. Phys.* **1974**, *61*, 2896.
(26) Schaefer, J.; Sefcik, M. D.; Stejskal, E. O.; McKay, R. A. *Macromolecules* **1981**, *14*, 188.
(27) Gilson, D. F. R.; McDowell, C. A. *Mol. Phys.* **1961**, *4*, 125.
(28) Woessner, D. *J. Chem. Phys.* **1961**, *35*, 41.
(29) Deutch, J. M.; Oppenheim, I. *Adv. Magn. Reson.* **1968**, *3*, 43.
(30) Cheung, T. T. P.; Yaris, R. *J. Chem. Phys.* **1980**, *72*, 3604.
(31) Demco, D. E.; Tegenfeldt, J.; Waugh, J. S. *Phys. Rev. B*, **1975**, *11*, 4133.
(32) Schaefer, J.; Stejskal, E. O.; Buchdahl, R. *J. Macromol. Sci., Phys.* **1977**, *B13*, 665.

Double-Cross-Polarization Detection of Labeled Chemical Bonds in HCN Polymerization

R. A. McKay, Jacob Schaefer,* and E. O. Stejskal

Physical Sciences Center, Monsanto Company, St. Louis, Missouri 63167

Robert Ludicky and C. N. Matthews

Department of Chemistry, University of Illinois at Chicago, Chicago, Illinois 60680.

Received July 29, 1983

ABSTRACT: Hydrogen cyanide reacts in the presence of base to form a complex mixture of HCN polymers. The structure of these polymers and the mechanism of their formation, especially the insoluble, higher molecular weight ones, have been disputed. It is of particular interest to know whether significant amounts of heteropolypeptides are present in these materials following hydrolysis in cold water. We have used CPMAS ^{15}N NMR previously to establish the presence of amide nitrogens in the insoluble hydrolysate. Now we report the use of double-cross-polarization (DCP) NMR to show that most of these nitrogens are found in peptide linkages. DCP NMR involves the sequential transfer of spin polarization from ^{1}H to ^{15}N to ^{13}C followed by the detection of ^{15}N under MAS conditions. The ^{15}N to ^{13}C transfer requires strong dipolar coupling between the spins and hence detects ^{15}N–^{13}C chemical *bonds* when compared with CPMAS ^{15}N NMR. Reactions of $H^{13}C^{15}N$ and $H^{12}C^{14}N$ *or* $H^{13}C^{14}N$ and $H^{12}C^{15}N$ to form $(HCN)_x$ have been examined with DCP NMR to detect the making or breaking of ^{15}N–^{13}C bonds to find evidence for peptide linkages and other structures.

Introduction

The combination of high-power resonant decoupling and high-speed mechanical sample spinning at the magic angle has been shown to produce liquidlike, high-resolution ^{13}C and ^{15}N NMR spectra of organic solids.[1-3] The sensitivity of these rare-spin NMR experiments is improved by cross-polarization transfer of spin polarization from the abundant protons to the rare spins.[4] One of the principal

0024-9297/84/2217-1124$01.50/0